Biophysical Journal Volume 75 December 1998 3120–3126

Electric Signals during the Bacteriorhodopsin Photocycle, Determined over a Wide pH Range

Krisztina Ludmann, Csilla Gergely, András Dér, and György Váró
Institute of Biophysics, Biological Research Centre of the Hungarian Academy of Sciences, Szeged H-6701, Hungary

ABSTRACT From the electric signals measured after photoexcitation, the electrogenicity of the photocycle intermediates of bacteriorhodopsin were determined in a pH range of 4.5–9. Current measurements and absorption kinetic signals at five wavelengths were recorded in the time interval from 300 ns to 0.5 s. To fit the data, the model containing sequential intermediates connected by reversible first-order reactions was used. The electrogenicities were calculated from the integral of the current signal, by using the time-dependent concentrations of the intermediates, obtained from the fits. Almost all of the calculated electrogenicities were pH independent, suggesting that the charge motions occur inside the protein. Only the N intermediate exhibited pH-dependent electrogenicity, implying that the protonation of Asp^{96}, from the intracellular part of the protein, is not from a well-determined proton donor. The calculated electrogenicities gave good approximations of all of the details of the measured electric signals.

INTRODUCTION

Bacteriorhodopsin (BR) is a light-driven proton pump found in the purple membrane (PM) of the cell membrane of *Halobacterium salinarum.* The energy of a light quantum absorbed by the all-*trans* retinal, bound to the Lys^{216} of the protein, is used to transport a proton from the cytoplasmic to extracellular regions of the cell (Lozier et al., 1975). Although a great deal of information is available about the protein sequence (Khorana et al., 1979; Ovchinnikov et al., 1979), the three-dimensional structure (Henderson et al., 1990; Grigorieff et al., 1996; Kimura et al., 1997), the structural changes during the function of BR (Subramaniam et al., 1993; Song et al., 1996), and the details of the charge motions during proton translocation are still unknown (for reviews see Stoeckenius et al., 1979; Lanyi, 1992; Ebrey, 1993; Lanyi and Váró, 1995).

Whereas the dark-adapted BR contains a mixture of all-*trans*, 15-*anti* and 13-*cis*, 15-*syn* retinal in thermal equilibrium, the light-adapted BR contains only all-*trans*, 15-*anti* retinal. After light excitation, both retinal conformations exhibit a photocycle (Lozier et al., 1992), but only the all-*trans* retinal containing BR has proton transport activity. The transporting photocycle goes through a series of spectrally different intermediate states (denoted by letters: K, L, M, N and O), and almost every intermediate has been divided into several spectrally silent substates (Váró and Lanyi, 1990; Zimányi et al., 1993; Cao et al., 1993; Gergely et al., 1993; Ganea et al., 1995; Friedman et al., 1994).

Although different models can describe the photocycle of BR, the two most accepted in the literature are the model with two or more parallel or branched photocycles, containing unidirectional reactions between the intermediates (Dancsházy et al., 1988; Drachev et al., 1993; Eisfeld et al., 1993; Song et al., 1994; Luchian et al., 1996), and the model with reversible reactions in a single photocycle, leading to transient equilibria between the intermediates (Ames and Mathies, 1990; Váró and Lanyi, 1990; Lozier et al., 1992; Druckmann et al., 1993; Hessling et al., 1993). For the wild-type and mutant BR it was shown that the sequential model with reversible reactions fits the absorption kinetic measurements better (Váró and Lanyi, 1990; Dér et al., 1992; Gergely et al., 1993), and the rate constants display linear Eyring plots, giving physically correct thermodynamic parameters for the reactions (Váró and Lanyi, 1991; Ludmann et al., 1998). In the present study we would like to interpret the measured absorption kinetic and electric signals, based on the sequential model with reversible reactions.

To measure the electric response signal of a light-activated protein such as BR, it is important to have an electrically anisotropic sample containing oriented proteins. Oriented samples can be obtained by incorporating BR into a bilayer lipid membrane (Dancsházy and Karvaly, 1976; Bamberg et al., 1981; Butt et al., 1989), or by oriented attachment of PM to a lipid-impregnated filter (Drachev et al., 1984) or a thin teflon sheet (Holz et al., 1988). These techniques are very sensitive to the electric signal measurement, but they have several drawbacks, because the membranes form a monolayer on the surface of the support. The very small optical density of the sample makes the absorption kinetic measurement rather difficult; therefore it is hard to establish any relationship between the electric signal components and photocycle intermediates. The two sides of the PMs are not equally accessible to the bathing suspension, and the measuring conditions are not well controlled over the whole sample. A large gradient can accumulate between the supporting membrane and the PM sheets, which can be controlled only by adding ionophores to the solution.

Received for publication 18 March 1998 and in final form 26 August 1998.
Address reprint requests to Dr. György Váró, Institute of Biophysics, Biological Research Centre of the Hungarian Academy of Science, Szeged, Temesvari KRT 62, H-6701, Hungary. Tel.: 36-62-432232; Fax: 36-62-433133; E-mail: varo@everx.szbk.u-szeged.hu.

0006-3495/98/12/3120/07 $2.00

When the role of internal water was investigated, the electrophoretic deposition of the PMs on a conducting glass surface gave oriented dried samples (Váró, 1981; Váró and Keszthelyi, 1983; Kononenko et al., 1986; Lewis et al., 1996). It was possible to carry out both electric and absorption kinetic measurements. The samples are very stable for years, which is important in technical applications, but such dried samples are far from the conditions of the living cell.

Another possibility is to apply an external electric field to the PM suspension, orienting the membrane fragments by their permanent dipole moment (Keszthelyi and Ormos, 1983; Keszthelyi and Ormos, 1989). The orientation can be fixed when the membranes are incorporated in an acrylamide gel and an external electric field is applied during the polymerization of the gel (Dér et al., 1985). Both absorption kinetic and electric signal measurements can be performed, and the bathing solution can easily be changed. This sample eliminates all of the problems of the earlier methods but has limitations at high salt concentrations, where the sample resistance is low, resulting in a decreased signal-to-noise ratio (Dér et al., 1988; Dér et al., 1992; Gergely et al., 1993).

The first attempt to interpret the electric signals showed a strong correlation between its components and the photocycle intermediates (Keszthelyi and Ormos, 1980; Keszthelyi and Ormos, 1983). The pH and salt concentration dependence of the electric signals was studied (Ormos et al., 1985; Liu, 1990; Liu et al., 1990). It was observed that some buffers at low concentration change the sign of the electric signals (Tóth-Boconádi et al., 1986; Dér et al., 1988; Liu et al., 1991). On the bases of the assumptions that only one proton moves and the dielectric constant of the protein is constant, a charge displacement distance was calculated for every intermediate (Keszthelyi and Ormos, 1980). During the photocycle not only the transported proton, but some charged amino acid side chains can also move, and there is no information about the local dielectric constant of the protein. Relative electrogenicity of the intermediates (Trissl, 1990; Gergely et al., 1993), as the change of the dipole magnitude relative to the ground state BR, is a more generalized description of the charge motions. The relative electrogenicities of the early intermediates have been determined on several mutant BRs (D85N, D212N, and D96N) (Gergely and Váró, 1992; Gergely et al., 1993; Ganea et al., 1995).

In the present study, the relative electrogenicities of the wild-type BR photocycle intermediates were studied in the pH range 4.5–9. From the pH dependence of the electrogenicities, conclusions were drawn about the charge motions occurring during the photocycle.

MATERIALS AND METHODS

Purple membranes were isolated from *Halobacterium salinarum* strain S9 by a standard procedure (Oesterhelt and Stoeckenius, 1974). Oriented purple membranes were immobilized in a polyacrylamide gel following the method of Dér et al. (1985), with a BR concentration of ~30 μM. To get a reasonable signal-to-noise ratio, a relatively low salt concentration was used. The thoroughly washed gels were soaked overnight in 50 mM NaCl, 12.5 mM 2-(*N*-morpholino)ethanesulfonic acid, 12.5 mM Tris buffer at the desired pH. This salt concentration had to be kept to avoid the problem of a large difference between the bulk and surface pH, observed at very low ionic strength (Szundi and Stoeckenius, 1989), which could lead to uncertainty of the pH of the measurement. The sample was kept overnight in the bathing solution to equilibrate the pH and salt concentration gradients. Before the measurement, the sample was placed in the sample holder and allowed to adjust to the required temperature, which ensured a good stability and reproducibility of the signal up to several hundred milliseconds. The electric and absorption kinetic measurements were performed at 20°C with a set-up described elsewhere (Váró and Keszthelyi, 1983; Ludmann et al., 1998). Data were recorded, after laser excitation of the sample on a linear time scale, and converted to a logarithmic time scale, covering the 300 ns to 0.5 s interval (Gergely et al., 1993). The linear-to-logarithmic conversion was accomplished by averaging the linear time points between two logarithmic time points, which improved the signal-to-noise ratio at later time points.

A complete set of data consists of absorption kinetic and electric signals measured at each pH. The analysis of the absorption kinetic data, measured at five wavelengths (410, 500, 570, 620, and 650 nm), was performed with the RATE program (Gergely et al., 1993; Váró et al., 1995; Ludmann et al., 1998). The calculated concentrations of the intermediates were used to fit the electric signal. The integral of the measured current signal, which is proportional to the voltage generated on the membrane, is given by the relation

$$U(t) = A * \sum_{\mathrm{i}} C_{\mathrm{i}}(t) * E_i \qquad (1)$$

where $U(t)$ is the voltage, A is a constant determined by the measuring conditions, E_{i} is the electrogenicity, and C_{i} is the concentration of the intermediate i. The electrogenicity of the intermediates was defined earlier (Trissl, 1990; Gergely et al., 1993) as the change in the dipole magnitude of the intermediate relative to the ground state. The electric signals arise only from the dipole magnitude changes in the direction perpendicular to the membrane. The sign of the electrogenicity is considered positive when the change in dipole moment is equivalent to a shift of a positive charge in the proton transporting direction of the membrane. The fit of the electric signals was carried out with the MATLAB program, version 4.2c.

RESULTS

To achieve a reliable electric signal analysis, the exact time constants and the time course of the concentration of intermediates had to be calculated. A representative set of signals, measured at pH 7, is presented in Fig. 1. Each chosen wavelength was primarily characteristic for one of the intermediates of the photocycle. The current signal (I) and its integral, the voltage (U), are generated by the charge motions occurring inside the membrane, during the whole photocycle. Whereas the fast part of the signal is better characterized by the current signal, the slow charge motions, with much larger electrogenicities, make a larger contribution to the integral. The fitting procedure was performed on the voltage signals.

Above pH 7, a characteristic peak appears in the current signal in the hundred nanosecond time interval (Fig. 2). In this time domain, there is not a large change in the absorption kinetic signals (not shown); only an acceleration of the rise of the M intermediate can be observed. In the voltage signal, the negative phase disappears earlier, with increasing

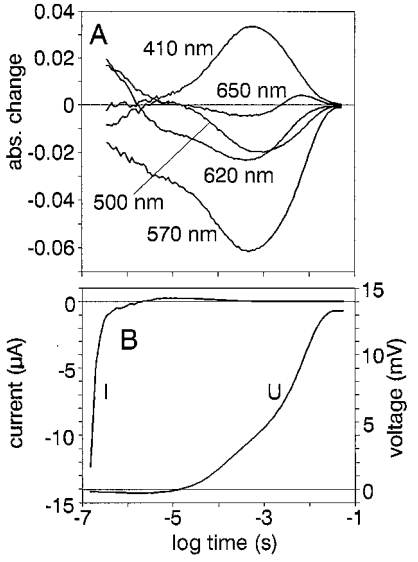

FIGURE 1 (*A*) Absorption kinetic measured at five wavelengths and (*B*) electric current (*I*) and its integral, the voltage signal (*U*), on a gel sample. Measuring conditions: 50 mM NaCl, 12.5 mM 2-(*N*-morpholino)ethanesulfonic acid, 12.5 mM Tris, pH 7, 20°C.

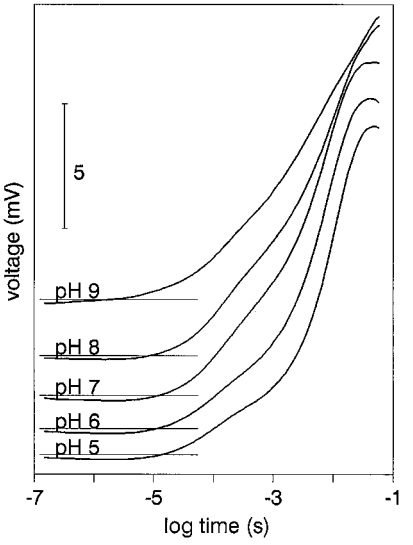

FIGURE 3 The pH dependence of the voltage signal. The measuring conditions are similar to Fig. 1, only at different pH values. The thin line at the beginning of the signals shows the value of the 0 voltage.

pH, and the late part of the voltage signal rises more slowly, as the whole photocycle becomes slower (Fig. 3).

For data analysis, the optical signals were fitted to the model containing the intermediates sequentially connected by thermally driven, first-order reversible reactions with branching at N intermediate (Váró and Lanyi, 1990; 1991). The model contains a unidirectional reaction only at the end of photocycle:

$$K \leftrightarrow L \leftrightarrow M_1 \leftrightarrow M_2 \leftrightarrow N \leftrightarrow O \rightarrow BR \quad \text{and} \quad N \rightarrow BR$$

All of the details of the photocycle are explained in the previous paper of this series (Ludmann et al., 1998). The extinction coefficients of the intermediates at the five selected wavelengths were taken from the literature (Gergely et al., 1997). The fits were good over the whole pH range.

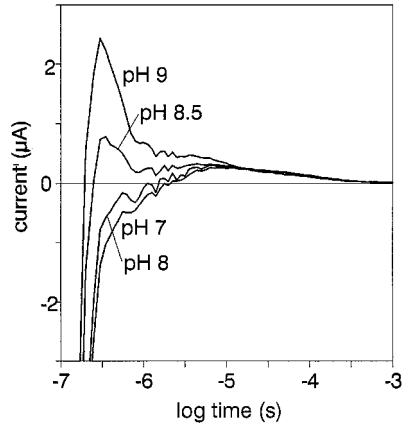

FIGURE 2 The pH dependence of the early part of the current signal. The measuring conditions are similar to Fig. 1, only at different pH values.

For example, the fit to the absorption kinetic measurement at pH 7 is presented in Fig. 4 *A*. The time-dependent concentrations of the intermediates (Fig. 4 *B*) were used to determine the electrogenicity of each intermediate, through Eq. 1. As the number of time points is much larger than the

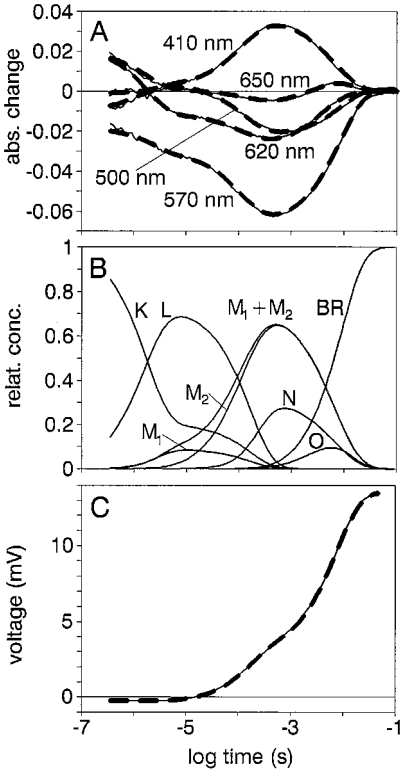

FIGURE 4 The fit to the absorption kinetic (*A*), the time course of the concentration of intermediates (*B*), and the fit to the voltage signal (*C*). The measured data at pH 7 are those shown in Fig 1.

number of the unknown electrogenicities, the system of equations was overdetermined. The solution was calculated by the least-squares method with the MATLAB program. The fast part of the photocycle contains electrogenicities smaller by one order of magnitude than the slow part. To avoid large errors in the electrogenicities for these early intermediates, the calculation was done in two steps. Initially, the first part of the voltage signal was fitted when only K, L, and M_1 intermediates were present. Then, fixing the obtained values, we determined the electrogenicity of the other intermediates, using the whole voltage signal. The calculated values of the electrogenicity were fitted back to the voltage signal and were in accordance (Fig. 4 *C*). The electrogenicity values of all of the intermediates, other than intermediate N, were constant over the studied pH range, within the ±15% error of determination (Fig. 5).

As a control for the early intermediates, the theoretical value of the current was calculated in the first five points of the measurement by multiplying the derivative of the concentrations by the electrogenicity of intermediates. At 250 ns after excitation, the values of the measured current signal and the theoretically calculated signal were normalized at the two extreme pH values. The agreement between the theoretical and experimental points (Fig. 6) indicates that the calculated electrogenicities describe the positive peak, appearing in the current at high pH values, shown in Fig. 2.

DISCUSSION

The combined absorption kinetic and electric signal measurements (Fig. 1), uniquely characteristic for the gel samples, allow correlation between the course of the electric signal and the photocycle intermediates. The pH-dependent changes in the current signal (Fig. 2) and voltage signal (Fig. 3) suggest that the charge motions inside the protein are strongly pH dependent. The appearance of the positive peak above pH 8 (Fig. 2) appears to be a titration of a charge. At longer times the voltage signal does not change dramatically but can be observed to alter continuously.

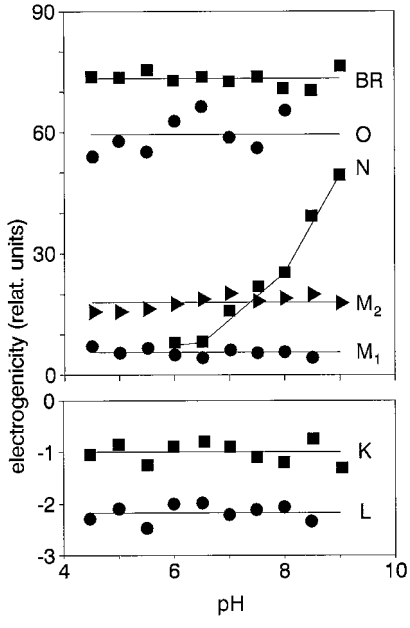

FIGURE 5 The pH dependence of the electrogenicities of the intermediates. The horizontal lines are the average value of the corresponding electrogenicities. The errors of calculation are less than ±15%.

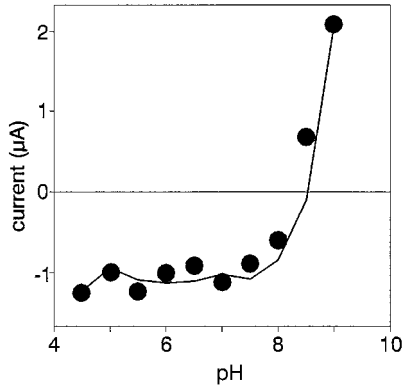

FIGURE 6 Comparison of the measured and calculated values of the positive signal appearing at high pH. Two hundred fifty nanoseconds after excitation the measured point of the current signal (*symbols*) and the theoretically calculated values of the same point (*line*) are normalized in the two extreme pH values.

The simultaneous fitting of the signals (Fig. 4) allows calculation of the electrogenicity of all of the intermediates. Except for the N intermediate, all of the electrogenicities were pH independent, within the error of calculation (Fig. 5). This suggests that none of the electrogenicities are titratable in this pH range. As the measured pH range is rather large, this implies that besides the transported proton, the charge motions are produced by side chains deep inside the protein or reorientation of several bound water molecules inside the proton channel that are not directly accessible from the aqueous phase. The study of the early intermediates, by the use of mutants D85N, D212N, and D96N, gave similar values for the electrogenicity of K, L, and M_1 and showed that they are pH independent (Gergely et al., 1993, 1995; Gergely and Váró, 1992). In the early steps, up to intermediate K, a charge separation along the retinal and the all-*trans* to 13-*cis* isomerization occur (Chang et al., 1985). The first negative electrogenicity arises from these processes. During the L intermediate, a local relaxation of the protein is observed (Lohrmann and Stockburger, 1992), involving some charged side chains, resulting in its negative electrogenicity. The L-to-M_1 transition contains an active proton translocation from the Schiff base to the proton acceptor Asp^{85} (Butt et al., 1989), giving a positive electrogenicity for intermediate M_1. The M_1-to-M_2 transition is considered as a conformational change of the protein, consisting in the tilt of the F and G helices almost parallel to the membrane, but there is a total shift in the positive charge toward the extracellular side of the membrane, resulting in the positive electrogenicity of intermediate M_2. This could be a combination of the proton motion on its pathway and

the projection on the membrane normal of the charge shift during the conformation change.

In the literature, not only M, but intermediates L, N, and O are also divided into substates (Zimányi et al., 1993; Cao et al., 1993; Gergely et al., 1993). In the present study, these "silent" transitions were not taken into account; during the calculation of the electrogenicities, only the overall electrogenicities of the intermediates were found. The transition through the N and O intermediates contains two major steps, the reprotonation of the Schiff base from Asp^{96} and the proton uptake step from the cytoplasmic half-channel of the membrane to Asp^{96} (Zimányi et al., 1993).

The electrogenicity of the intermediate O has a large positive value and is pH independent. At low pH, when no N but O is present in the photocycle, enough protons are still present to reprotonate Asp^{96} from the same distance, and the rate-limiting step is the reisomerization of the retinal. At high pH values, the reprotonation goes together with the intermediate N, and the intermediate O kinetically disappears from the photocycle, indicating that the rate-limiting step is related to the proton translocation process. Around pH 6, both intermediates N and O are present in a rather low concentrations. The fit of the N and O intermediates to the electric signal contains a large error when their concentration is low (see the electrogenicity of the O in Fig. 5). The very low electrogenicity of intermediate N is compensated by a corresponding high value for O.

The change in the electrogenicity of the intermediate N at high pH values seems to be highly pH dependent. It is possible that when the pH rises the probability of taking up a proton from the surrounding decreases. The proton should come from a greater distance in the cytoplasmic half-channel. This suggests that there is not a well-determined location of a proton donor for Asp^{96}, but the conformational changes of the protein and the available free proton in the cytoplasmic half-channel modulate its accessibility (Zimányi et al., 1993; Brown et al., 1995). When Asp^{96} is replaced by Asn, reprotonation of the Schiff base becomes pH dependent, the proton donor is missing, and the reprotonation takes place in a manner similar to that of the reprotonation of Asp^{96} in wild-type BR. In the mutant D96N, the electrogenicity of the intermediate M_2 becomes pH dependent (Gergely et al., 1993). This could reflect a pH-dependent change in the protonation state of an amino acid side chain or water in the intracellular half-channel, during the conformation change of the protein. Another explanation of the pH dependency of the electrogenicity of the intermediate N may be due to the fact that only one N intermediate was considered. It is known that two kinetically strongly overlapping N's exist with different protonations of the protein (Zimányi et al., 1993). They may have different electrogenicities. With increasing pH, the equilibrium between the two substates changes, resulting in a changing electrogenicity of the global N intermediate.

At the end of the photocycle, the protein returns to the unexcited ground-state BR. As the ion strength of the suspension is kept constant, there is no change in the thickness of the membrane and the double layer at the surface. The electrogenicity value of BR is given solely by the translocation of the proton from one side of the membrane to the other, which, on the basis of the above-mentioned constancy of the membrane thickness, should be constant, a requirement fulfilled by the calculations (see Fig. 5).

A verification of the reliability of the electrogenicity values is the fit of the calculated voltage signals to the measured ones (Fig. 4 *C*) and the fit of the theoretically calculated current at 250 ns to the measured currents (Fig. 6). It is important to note that no titration of the electrogenicity need be considered, as the change in the kinetic constants describes the whole effect.

This study proved that the electrogenicity of the photocycle intermediates, with the exception of the N intermediate, are pH independent. This indicates that the charge motions inside the protein, during the proton transport steps, are the same for the whole studied pH range. The location of charge transfer, during a particular transition between the intermediates, is pH independent; hence the charge configuration of each intermediate is pH independent. The electric measurements do not give information about the proton release or uptake step but show that the transfer of protons from one side of the membrane to the other occurs in well-determined steps. The constancy of the electrogenicities can be regarded as another indirect proof of the validity of the considered photocycle.

The authors are grateful to Prof. L. Keszthelyi and Prof. J. K. Lanyi for helpful discussions.

This work was supported by a grant from the National Science Research Fund of Hungary (OTKA T022066) and the Academic Research Fund of the Hungarian Academy of Sciences (97-71, 3, 3/52).

REFERENCES

Ames, J. B., and R. A. Mathies. 1990. The role of back-reactions and proton uptake during the N→O transition in bacteriorhodopsin's photocycle: a kinetic resonance Raman study. *Biochemistry.* 29: 7181–7190.

Bamberg, E., N. A. Dencher, A. Fahr, and M. P. Heyn. 1981. Transmembranous incorporation of photoelectrically active bacteriorhodopsin in planar lipid bilayers. *Proc. Natl. Acad. Sci. USA.* 78:7502–7506.

Brown, L. S., G. Váró, R. Needleman, and J. K. Lanyi. 1995. Functional significance of a protein conformation change at the cytoplasmic end of helix F during the bacteriorhodopsin photocycle. *Biophys. J.* 69: 2103–2111.

Butt, H.-J., K. Fendler, E. Bamberg, J. Tittor, and D. Oesterhelt. 1989. Aspartic acids 96 and 85 play a central role in the function of bacteriorhodopsin as a proton pump. *EMBO J.* 8:1657–1663.

Cao, Y., L. S. Brown, R. Needleman, and J. K. Lanyi. 1993. Relationship of proton uptake on the cytoplasmic surface and the reisomerization of the retinal in the bacteriorhodopsin photocycle: an attempt to understand the complex kinetics of the protons and the N and O intermediates. *Biochemistry.* 32:10239–10248.

Chang, C.-H., R. Govindjee, T. G. Ebrey, K. Bagley, G. Dollinger, L. Eisenstein, J. Marque, H. Roder, J. Vittitow, and J. M. Fang. 1985. *Trans*/13-*cis* isomerization is essential for both the photocycle and proton pumping of bacteriorhodopsin. *Biophys. J.* 47:509–512.

Dancsházy, Z., R. Govindjee, and T. G. Ebrey. 1988. Independent photocycles of the spectrally distinct forms of bacteriorhodopsin. *Proc. Natl. Acad. Sci. USA.* 85:6358–6361.

Dancsházy, Z., and B. Karvaly. 1976. Incorporation of bacteriorhodopsin into a bilayer lipid membrane; a photoelectric-spectroscopic study. *FEBS. Lett.* 72:136–138.

Dér, A., P. Hargittai, and J. Simon. 1985. Time-resolved photoelectric and absorption signals from oriented purple membranes immobilized in gel. *J. Biochem. Biophys. Methods.* 10(5–6):295–300.

Dér, A., R. Tóth-Boconádi, and L. Keszthelyi. 1988. Counterions and the bacteriorhodopsin proton pump. *FEBS Lett.* 229:313–316.

Dér, A., R. Tóth-Boconádi, and S. Száraz. 1992. Electric signals, and the photocycle of bacteriorhodopsin. *In* Structures and Functions of Retinal Proteins. J. L. Rigaud, editor. John Libbey and Co., London. 197–200.

Drachev, L. A., A. D. Kaulen, and A. Y. Komrakov. 1993. On the two pathways of the M-intermediate formation in the photocycle of bacteriorhodopsin. *Biochem. Int.* 30:461–469.

Drachev, L. A., A. D. Kaulen, and V. P. Skulachev. 1984. Correlation of photochemical cycle, H^+ release and uptake, and electrical events in bacteriorhodopsin. *FEBS Lett.* 178:331–335.

Druckmann, S., M. P. Heyn, J. K. Lanyi, M. Ottolenghi, and L. Zimányi. 1993. Thermal equilibration between the M and N intermediates in the photocycle of bacteriorhodopsin. *Biophys. J.*

Ebrey, T. G. 1993. Light energy transduction in bacteriorhodopsin. *In* Thermodynamics of Membranes, Receptors and Channels. M. Jackson, editor. CRC Press, Boca Raton, FL. 353–387.

Eisfeld, W., C. Pusch, R. Diller, R. Lohrmann, and M. Stockburger. 1993. Resonance Raman and optical transient studies on the light-induced proton pump of bacteriorhodopsin reveal parallel photocycles. *Biochemistry.* 32:7196–7215.

Friedman, N., Y. Gat, M. Sheves, and M. Ottolenghi. 1994. On the heterogeneity of the M population in the photocycle of bacteriorhodopsin. *Biochemistry.* 33:14758–14767.

Ganea, C., C. Gergely, and G. Váró. 1995. Substates in bacteriorhodopsin photocycle. *Electro. Magnetobiol.* 14:229–241.

Gergely, C., C. Ganea, G. I. Groma, and G. Váró. 1993. Study of the photocycle and charge motions of the bacteriorhodopsin mutant D96N. *Biophys. J.* 65:2478–2483.

Gergely, C., C. Ganea, S. Száraz, and G. Váró. 1995. Charge motions studied in the bacteriorhodopsin mutants D85N and 12N. *Photochem. Photobiol. B Biol.* 27:27–32.

Gergely, C., and G. Váró. 1992. Charge motions in the D85N, and D212N mutants of bacteriorhodopsin. *In* Structures and Functions of Retinal Proteins. J. L. Rigaud, editor. John Libbey Eurotext, London. 193–196.

Gergely, C., L. Zimányi, and G. Váró. 1997. Bacteriorhodopsin intermediate spectra determined over a wide pH range. *J. Phys. Chem.*

Grigorieff, N., T. A. Ceska, K. H. Downing, J. M. Baldwin, and R. Henderson. 1996. Electron-crystallographic refinement of the structure of bacteriorhodopsin. *J. Mol. Biol.* 259:393–421.

Henderson, R., J. M. Baldwin, T. A. Ceska, F. Zemlin, E. Beckmann, and K. H. Downing. 1990. Model for the structure of bacteriorhodopsin based on high-resolution electron cryo-microscopy. *J. Mol. Biol.* 213: 899–929.

Hessling, B., G. Souvignier, and K. Gerwert. 1993. A model-independent approach to assigning bacteriorhodopsin's intramolecular reactions to photocycle intermediates. *Biophys. J.* 65:1929–1941.

Holz, M., M. Lindau, and M. P. Heyn. 1988. Distributed kinetics of the charge movements in bacteriorhodopsin: evidence for conformational substates. *Biophys. J.* 53:623–633.

Keszthelyi, L., and P. Ormos. 1980. Electric signals associated with the photocycle of bacteriorhodopsin. *FEBS Lett.* 109:189–193.

Keszthelyi, L., and P. Ormos. 1983. Displacement current on purple membrane fragments oriented in a suspension. *Biophys. Chem.* 18: 397–405.

Keszthelyi, L., and P. Ormos. 1989. Protein electric response signals from dielectrically polarized systems. *J. Membr. Biol.* 109:193–200.

Khorana, H. G., G. E. Gerber, W. C. Herlihy, C. P. Gray, R. J. Anderegg, K. Nihei, and K. Biemann. 1979. Amino acid sequence of bacteriorhodopsin. *Proc. Natl. Acad. Sci. USA.* 76:5046–5050.

Kimura, Y., D. G. Vassylyev, A. Miyazawa, A. Kidera, M. Matsushima, K. Mitsuoka, K. Murata, T. Hirai, and Y. Fujiyoshi. 1997. Surface of bacteriorhodopsin revealed by high-resolution electron crystallography. *Nature.* 389:206–211.

Kononenko, A. A., E. P. Lukashev, A. V. Maximychev, S. K. Chamorovsky, A. B. Rubin, S. F. Timashev, and L. N. Chekulaeva. 1986. Oriented purple membrane films as a probe for studies of the mechanism of bacteriorhodopsin functioning. I. The vectorial character of the external electric-field effect on the dark state and the photocycle of bacteriorhodopsin. *Biochim. Biophys. Acta.* 850:162–169.

Lanyi, J. K. 1992. Proton transfer and energy coupling in the bacteriorhodopsin photocycle. *J. Bioenerg. Biomembr.* 24:169–179.

Lanyi, J. K., and G. Váró. 1995. The photocycle of bacteriorhodopsin. *Isr. J. Chem.* 35:365–385.

Lewis, A., I. Rousso, E. Khachatryan, I. Brodsky, K. Lieberman, and M. Sheves. 1996. Directly probing rapid membrane protein dynamics with an atomic force microscope: a study of light-induced conformational alterations in bacteriorhodopsin. *Biophys. J.* 70:2380–2384.

Liu, S. Y. 1990. Light-induced currents from oriented purple membrane. I. Correlation of the microsecond component (B2) with the L-M photocycle transition. *Biophys. J.* 57:943–950.

Liu, S. Y., R. Govindjee, and T. G. Ebrey. 1990. Light-induced currents from oriented purple membrane. II. Proton and cation contributions to the photocurrent. *Biophys. J.* 57:951–963.

Liu, S. Y., M. Kono, and T. G. Ebrey. 1991. Effect of pH buffer molecules on the light-induced currents from oriented purple membrane. *Biophys. J.* 60:204–216.

Lohrmann, R., and M. Stockburger. 1992. Evidences for structural changes at the chromophoric site of bacteriorhodopsin during the K-to-L transition. 221:147–150 (Abstr.).

Lozier, R. H., R. A. Bogomolni, and W. Stoeckenius. 1975. Bacteriorhodopsin: a light-driven proton pump in *Halobacterium halobium. Biophys. J.* 15:955–963.

Lozier, R. H., A. Xie, J. Hofrichter, and G. M. Clore. 1992. Reversible steps in the bacteriorhodopsin photocycle. *Proc. Natl. Acad. Sci. USA.* 89:3610–3614.

Luchian, T., Z. Tokaji, and Z. Dancsházy. 1996. Actinic light density dependence of the O intermediate of the photocycle of bacteriorhodopsin. *FEBS Lett.* 386:55–59.

Ludmann, K., C. Gergely, and G. Váró. 1998. I. Kinetic and thermodynamic study of the bacteriorhodopsin photocycle in a wide pH range. *Biophys. J.* 75:000–000.

Oesterhelt, D., and W. Stoeckenius. 1974. Isolation of the cell membrane of *Halobacterium halobium* and its fractionation into red and purple membrane. *Methods Enzymol.* 31:667–678.

Ormos, P., S. G. Hristova, and L. Keszthelyi. 1985. The effect of pH on proton transport by bacteriorhodopsin. *Biochim. Biophys. Acta.* 809: 181–186.

Ovchinnikov, Y. A., N. G. Abdulaev, M. Y. Feigina, A. V. Kiselev, and N. A. Lobanov. 1979. The structural basis of the functioning of bacteriorhodopsin: an overview. *FEBS Lett.* 100:219–224.

Song, L., S. L. Logunov, D. Yang, and M. A. El-Sayed. 1994. The pH dependence of the subpicosecond retinal photoisomerization process in bacteriorhodopsin: evidence for parallel photocycles. *Biophys. J.* 67: 2008–2012.

Song, Q., G. S. Harms, and C. K. Johnson. 1996. Chromophore reorientation relative to the membrane plane detected by time-resolved linear dichroism during the bacteriorhodopsin photocycle in oriented purple membrane. *J. Phys. Chem.* 100:15605–15613.

Stoeckenius, W., R. H. Lozier, and R. A. Bogomolni. 1979. Bacteriorhodopsin and the purple membrane of halobacteria. *Biochim. Biophys. Acta.* 505:215–278.

Subramaniam, S., M. Gerstein, D. Oesterhelt, and R. Henderson. 1993. Electron diffraction analysis of structural changes in the photocycle of bacteriorhodopsin. *EMBO J.* 12:1–8.

Szundi, I., and W. Stoeckenius. 1989. Surface pH controls purple-to-blue transition of bacteriorhodopsin. A theoretical model of purple membrane surface. *Biophys. J.* 56:369–383.

Tóth-Boconádi, R., S. G. Hristova, and L. Keszthelyi. 1986. Diamines reverse the direction on the bacteriorhodopsin proton pump. *FEBS Lett.* 195:164–168.

Trissl, H. W. 1990. Photoelectric measurements of purple membranes. *Photochem. Photobiol.* 51:793–818.

Váró, G. 1981. Dried oriented purple membrane samples. *Acta Biol. Acad. Sci. Hung.* 32:301–310.

Váró, G., and L. Keszthelyi. 1983. Photoelectric signals from dried oriented purple membranes of *Halobacterium halobium. Biophys. J.* 43: 47–51.

Váró, G., and J. K. Lanyi. 1990. Pathways of the rise and decay of the M photointermediate of bacteriorhodopsin. *Biochemistry.* 29:2241–2250.

Váró, G., and J. K. Lanyi. 1991. Thermodynamics and energy coupling in the bacteriorhodopsin photocycle. *Biochemistry.* 30:5016–5022.

Váró, G., R. Needleman, and J. K. Lanyi. 1995. Light-driven chloride ion transport by Halorhodopsin from *Natronobacterium pharaonis*. 2. Chloride release and uptake, protein conformation change, and thermodynamics. *Biochemistry.* 34:14500–14507.

Zimányi, L., Y. Cao, R. Needleman, M. Ottolenghi, and J. K. Lanyi. 1993. Pathway of proton uptake in the bacteriorhodopsin photocycle. *Biochemistry.* 32:7669–7678.